

# MODELLING VIRAL AND IMMUNE SYSTEM DYNAMICS

Alan S. Perelson

During the past 6 years, there have been substantial advances in our understanding of human immunodeficiency virus 1 and other viruses, such as hepatitis B virus and hepatitis C virus, that cause chronic infection. The use of mathematical modelling to interpret experimental results has made a significant contribution to this field. Mathematical modelling is also improving our understanding of T-cell dynamics and the quantitative events that underlie the immune response to pathogens.

## CD4 COUNT

A normal CD4 count is 1,000 per  $\mu\text{l}$ , with a range of 600–1,400 per  $\mu\text{l}$ . The count falls during primary infection, then returns to near or lower than normal levels. It then slowly falls, taking many years to reach the level of 200 per  $\mu\text{l}$  that characterizes AIDS.

The immune system is a complex system that can mount different types and intensities of responses, learn from experience and exhibit memory. Regulation in the immune system involves multiple cell types and probably hundreds of soluble mediators and different receptor–ligand interactions. Obtaining an integrated view of the immune system will entail the development of models that look at the immune system in various ways — some qualitative, some quantitative<sup>1</sup>. Although mathematical modelling has yielded some quantitative results that have improved our understanding of immunological phenomena<sup>2–17</sup>, it is still in its infancy. Successes in areas such as human immunodeficiency virus (HIV) dynamics, as well as the wealth of data coming from high-throughput experimental techniques, have provided a strong motivation for pursuing a quantitative approach. This review will focus on models of HIV and T-lymphocyte dynamics, and include more limited discussions of hepatitis C virus (HCV), hepatitis B virus (HBV), cytomegalovirus (CMV) and lymphocytic choriomeningitis virus (LCMV) dynamics and interactions with the immune system, highlighting the insights gained through modelling.

## HIV — a success story for modelling

HIV, on average, takes about 10 years to advance from initial infection to full-blown AIDS. If a patient with chronic HIV infection is repeatedly sampled and the viral load in plasma measured, the viral load generally remains unchanged. This suggested that the rate of HIV replication was very slow. During Phase I/II clinical trials

of one of the first HIV-1 protease inhibitors, **ritonavir**, in chronic HIV patients (mean CD4 COUNT = 180), the plasma level of HIV-1 RNA was observed to drop by one to two orders of magnitude during the first 2 weeks of therapy<sup>18–20</sup>. Although this, as well as earlier observations, indicated that the virus might be replicating rapidly, modelling the effects of drug therapy was able to quantify rates of virus production and loss, and indicated two important points. First, HIV-1 is cleared from chronically infected patients at a rapid rate, with the half-life of the virus in plasma estimated in this case to be 6 hours or less<sup>20</sup>. Second, to maintain a constant (or steady-state) level of virus in the plasma before therapy required that HIV-1 be produced at a rapid rate in these patients, with, on average, at least  $10^{10}$  virions being produced daily<sup>20</sup>. The experimental observations and quantitative estimates that followed strongly supported the idea that HIV-1 was a rapidly reproducing virus and one that could respond to therapy<sup>21,22</sup>. Furthermore, at the predicted rate of rapid HIV-1 production, one could mathematically show that during HIV-1 replication every single possible point mutation of the viral genome would be made hundreds or thousands of times each day<sup>21,23</sup>. So, modelling indicated that the virus could quickly become resistant to any single drug, particularly those that required one mutation to generate resistance.

## Viral dynamics

The basic ideas that drove the analysis of HIV-infection kinetics, and that led to the development of the field called viral dynamics<sup>24</sup>, are simple. First, in patients

*Theoretical Division,  
Los Alamos National  
Laboratory, MS-K710,  
Los Alamos,  
New Mexico 87545, USA.  
e-mail: asp@lanl.gov  
DOI: 10.1038/nri700*

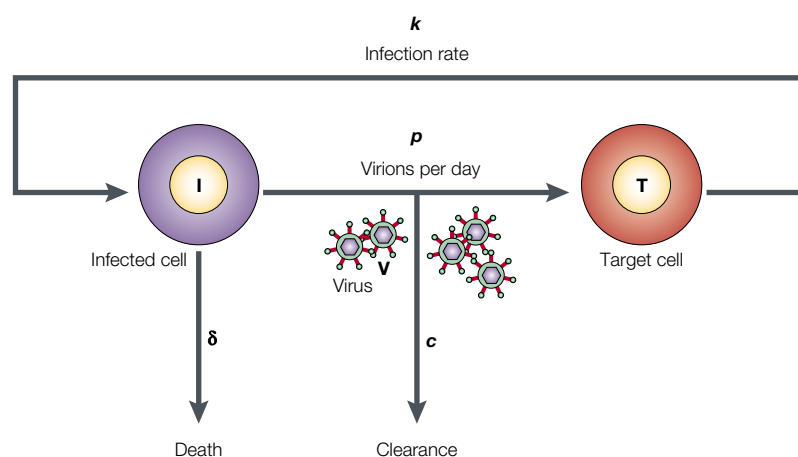


**Figure 1 | Basic model of viral infection.** Cells susceptible to infection, that is, target cells (T), are infected by virus (V) with rate constant  $k$ . Although not shown, target cells are assumed to be produced from a source at rate  $\lambda$ , and to die at rate  $d$  per cell. Infection produces productively infected cells (I), which produce new virions at rate  $p$ , and die at rate  $\delta$  per cell. Free virions are cleared at rate  $c$  per virion. This model and minor variants have been used to study the dynamics of human immunodeficiency virus, hepatitis C virus, hepatitis B virus and cytomegalovirus infections *in vivo*.

with chronic viral disease, the level of virus frequently reaches a constant or set-point level<sup>25</sup>, and then remains at approximately that level for years. To maintain this constant level the body must be producing and clearing virus at the same rate. If this were not the case, and, for example, more virus was produced each day than was cleared, then the amount of virus would slowly increase. Mathematically, if  $P$  is the total rate of virus production and  $c$  is the clearance rate per virion, then to maintain a viral set point,  $P$  must equal  $cV$ , where  $v$  is the viral load at the set point. If  $P > cV$ , then the viral load will increase; whereas, if  $P < cV$ , the viral load will decrease. At the set point  $P = cV$ , therefore, simply measuring the amount of virus at the set point,  $V$ , does not tell one whether the virus is produced slowly or rapidly. Second, the way to gain information on rates of viral production and clearance is to perturb the system. For example, if production is fully blocked, then the viral load will fall and the rate at which it falls is the clearance rate. If production is not fully blocked, then the rate of viral-load decline will depend not only on the virion-clearance rate, but also on the rate of death of virus-producing cells and the efficacy of the drug being used to block viral production. Last, fitting the kinetics of viral decay to mathematical models can elucidate the kinetic parameters governing viral infection, cell death and, in some cases, the efficacy of antiviral therapy.

### Basic model of virus infection

A model that has been used to study HIV, HCV and HBV infection is shown in FIG. 1. The model considers a set of cells susceptible to infection, that is, target cells,  $T$ , which, through interactions with virus,  $V$ , become infected. Infected cells,  $I$ , are each assumed to produce new virus particles at a constant average rate  $p$  and to die at rate  $\delta$  per cell. The average lifespan of a productively infected cell is  $1/\delta$ , and so if an infected

cell produces a total of  $N$  virions during its lifetime, the average rate of virus production per cell,  $p = N\delta$ . In the case of HIV infection, death might involve viral cytopathic effects or immune-mediated cellular destruction. Newly produced virus particles,  $V$ , can either infect new cells or be cleared from the body at rate  $c$  per virion. BOX 1 shows the equations<sup>26</sup> corresponding to the model in FIG. 1 and illustrates their use in analysing data obtained from HIV-infected individuals on antiretroviral therapy to obtain minimal estimates of the parameters  $c$  and  $\delta$ . From these estimates one can compute upper bounds for the half-life of virions in plasma ( $t_{1/2} = \ln 2/c$ ) and the half-life of productively infected cells ( $t_{1/2} = \ln 2/\delta$ ).

Although models and data-fitting techniques allow estimation of parameters characterizing viral infection, models can be wrong, errors in analysis can occur, different fitting methods can give different answers<sup>27</sup>, and multiple solutions (local optima) might confound NONLINEAR LEAST SQUARES or maximum-likelihood fitting. Therefore, it is important to independently confirm parameter estimates. In the presence of a 100% effective protease inhibitor, infectious virus production is inhibited, and infectious virus should decay exponentially with slope  $c$ . Measuring the rate of loss of viral infectivity was used by Perelson *et al.*<sup>20</sup> to confirm the estimate of  $c$  in one patient with high-baseline viral load. In other patients, infectivity decayed too rapidly to quantify. Another approach to estimating  $c$  is to use plasma apheresis<sup>28</sup>. In this technique, plasma with suspended virus is removed from a patient at a known rate, and fluids are returned to the patient to maintain blood volume. If the rate at which virus is removed by apheresis is small compared with  $cV$ —the rate of natural clearance—then apheresis will have little impact on plasma viral load. Conversely, if the rate of removal by apheresis is large compared with  $cV$ , the plasma virus concentration will fall. A model of apheresis was developed and data from apheresis experiments then used to estimate  $c$  (REF. 28). This approach confirmed that HIV was cleared rapidly; in four patients, the half-life of HIV varied between 28 min and 110 min, with a mean of  $\sim 1$  hour; whereas,  $c$  varied between 9.1 per day and 36 per day, with a mean of 23 per day (REF. 28).

Using the formula  $P = cV$ , and taking into account each patient's estimated plasma and extracellular fluid volume based on body weight, the total rate of virus production can be calculated. For HIV, estimates made in 1996 using a  $t_{1/2}$  of 6 hours for virus ( $c = 3$  per day), indicated that a minimum of  $10^{10}$  virions were produced daily<sup>20</sup>. That estimate might need to be revised upward by a factor of 8 or so given the apheresis-based estimate of  $c$ . On the basis of the rapid replication of HIV-1, its mutation rate ( $3.4 \times 10^{-5}$  per base per replication cycle<sup>29</sup>) and its genome size ( $\sim 10^4$  bases), one can compute that, on average, mutations will occur in every position in the genome multiple times each day and that a sizeable fraction of all possible double mutations will also occur each day<sup>23</sup>. Although treating cancer and some infectious diseases with multiple drugs is commonplace, the realization that HIV replicates and mutates rapidly provided a reason for treating HIV-infected patients with three or more drugs.

**V**  
Various notations have been used in modelling viral infections.  $V$ , the concentration of free virus, in the case of HIV, is measured in units of HIV-1 RNA per ml. As there are two RNAs per virion, the true concentration of virions is half the RNA concentration.

**I**  
Productively infected cells have here been denoted  $I$ . In the HIV literature, as there are different types of infected cells,  $T^*$ , has been used instead of  $I$  to denote the population of productively infected CD4<sup>+</sup> T cells. In the case of HCV and HBV,  $I$  denotes infected hepatocytes.

**NONLINEAR LEAST SQUARES**  
A procedure that estimates the parameters in a model by minimizing the differences between model predictions and data.

In clinical studies, when three or more drugs are given to HIV-infected patients, plasma virus decays with an initial rapid exponential decline of nearly 2 logs (first phase), followed by a slower exponential decline (second phase) that leads to the virus falling below levels of detection. The slope of the decline depends on the efficacy of the therapy, with faster declines corresponding

with more potent therapy<sup>26,30–32</sup>. This principle has been used to compare the efficacies of different drug doses<sup>33,34</sup> and different drug regimes<sup>35</sup>. To interpret the two-phase decline a new model was introduced<sup>36</sup>, which postulated that the second phase was due to sources of HIV-1 not included in the basic model. Candidates were a longer-lived population of productively infected cells,

### Box 1 | Modelling HIV dynamics

The equations that describe the basic model of viral dynamics shown in FIG. 1 are:

$$dT/dt = \lambda - dT - kVT \quad (1)$$

$$dI/dt = kVT - \delta I \quad (2)$$

$$dV/dt = pI - cV \quad (3)$$

If one assumes that initially a person is uninfected and then introduces a small amount of virus, the solution of equations 1–3 mimics the kinetics of primary human immunodeficiency virus (HIV) infection<sup>66</sup>. To analyse the effects of giving an antiretroviral drug, equations 1–3 are modified. Reverse transcriptase (RT) inhibitors block the ability of HIV to successfully infect a cell. Protease inhibitors (PI) cause the production of non-infectious viral particles,  $V_{NI}$ . So, in the presence of these drugs, the model equations become:

$$dT/dt = \lambda - dT - (1 - \varepsilon_{RT})kV_I T \quad (4)$$

$$dI/dt = (1 - \varepsilon_{RT})kV_I T - \delta I \quad (5)$$

$$dV_I/dt = (1 - \varepsilon_{PI})pI - cV_I \quad (6)$$

$$dV_{NI}/dt = \varepsilon_{PI}pI - cV_{NI} \quad (7)$$

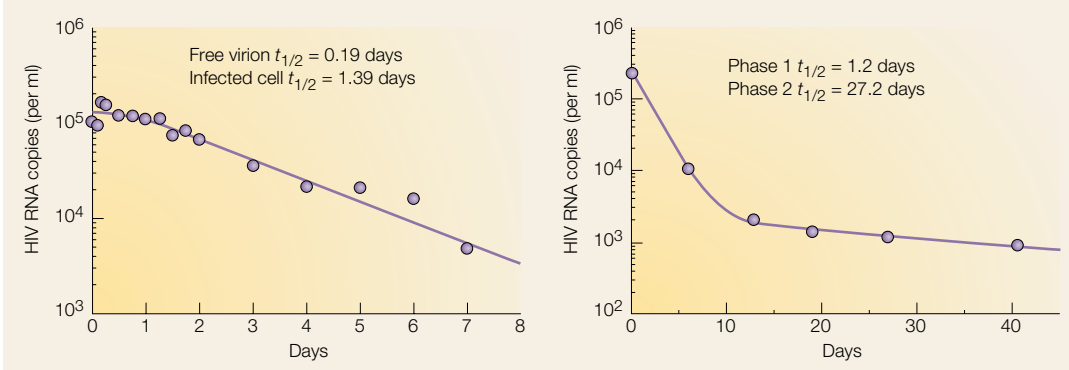
where  $\varepsilon_{RT}$  and  $\varepsilon_{PI}$  are the efficacies of RT and PI ( $\varepsilon = 1$  being a perfect drug),  $V_I$  and  $V_{NI}$  are the concentration of 'infectious' and 'non-infectious' virus, respectively,  $V = V_I + V_{NI}$  is the total amount of virus.

If a 100% effective PI is given to an individual at steady state with viral load,  $V_0$ , and one assumes that over the time period of interest  $T$  remains constant, the viral load decay will obey the equation<sup>20</sup>:

$$V(t) = V_0 \exp(-ct) + \frac{cV_0}{c - \delta} \cdot \left[ \frac{cV_0}{c - \delta} \{ \exp(-\delta t) - \exp(-ct) \} - \delta t \exp(-ct) \right] \quad (8)$$

Using nonlinear least-squares regression this equation was fitted to patient data and used to estimate the parameters  $c$  and  $\delta$ . The left graph shows data obtained from an HIV-infected patient who initiated antiretroviral therapy at time 0. The solid line is the best-fit theoretical curve from which the parameters  $c$  and  $\delta$  were estimated. (Reproduced with permission from REF. 20 © (1996) American Association for the Advancement of Science.)

To explain the results of longer-term combination therapy, more complex models were needed that postulated the existence of a second source of virus, such as long-lived infected cells<sup>36</sup>. The right graph shows data obtained from an HIV-infected patient who initiated combination antiretroviral therapy at time 0. The solid line is the best-fit theoretical curve from which model parameters and half-lives were estimated. (Reproduced with permission from REF. 36 © (1997) Macmillan Magazines Ltd.)



activation of latently infected cells and release into the blood of virions trapped in tissue reservoirs — for example, on FOLLICULAR DENDRITIC CELLS (FDCs). Models of all three processes fit experimental data on the rate of plasma virus decline equally well<sup>36</sup>, and therefore the cause of the second phase could not be discerned by modelling alone. Additional data, quantifying the density of productively infected plus latently infected cells that could be activated into productive infection were then collected from HIV-infected patients. Simultaneously, fitting viral load and infected cell declines indicated that activation of latently infected cells was unlikely to be an important source of second-phase virus, and that long-lived cells were projected to decay after 2–3 years of 100% effective therapy. Some incorrectly interpreted the predicted decay of long-lived cells to mean that HIV-1 could be eradicated from a patient in 2–3 years. This ‘eradication hypothesis,’ as it was called, turned out not to be true. It was shown that replication-competent virus could be isolated from infected patients despite prolonged plasma virus suppression during 3–4 years of antiretroviral treatment<sup>37</sup>. Resting CD4<sup>+</sup> memory T cells were identified as a long-lived latent reservoir<sup>38</sup>, and their mean half-life was estimated in different studies as being as short as 6 months<sup>39</sup> or as long as 43.9 months<sup>40–42</sup>. In either event, latently infected cells were decaying extremely slowly, and so possibly comprised a third phase of viral decay. Because current therapy does not seem to be 100% effective<sup>39,43–45</sup>, replenishment of this reservoir could be due to low-level ongoing replication<sup>46</sup>. Mathematical models of the release of HIV-1 virions attached to FDCs, assuming virions do not degrade, indicated that a small fraction of virions could remain attached for over a decade<sup>47</sup> and that their rate of release was compatible with two-phase decay of plasma virus<sup>48,49</sup>. Experiments in mice showed that HIV-1 attached to FDCs could remain infectious for 9 months<sup>50</sup>, raising the possibility that retention of virions on FDCs, as well as the slow decay of latently infected cells, could hinder the eradication of HIV and drive the need for life-long therapy.

### Modelling other viruses

The ‘basic’ model (FIG. 1) used to study HIV viral dynamics has been applied to understand the kinetics of HCV, HBV and CMV — other viruses that can cause chronic infection.

**HCV.** Treatment of HCV with high daily doses of INTERFERON- $\alpha$  (IFN- $\alpha$ ), can cause the viral load to decrease by two orders of magnitude in the first day of treatment<sup>51–54</sup>. A similar decline in HIV levels takes 1–2 weeks using potent combination therapy — why the difference? Modelling has provided a testable hypothesis: IFN- $\alpha$ , by a direct antiviral effect, causes infected cells to rapidly reduce their rate of viral production<sup>51</sup>. As indicated by the basic model (FIG. 1), if IFN- $\alpha$  reduces production, then viral clearance can rapidly reduce the amount of HCV in serum. If IFN- $\alpha$  increased  $c$ , then a similar rapid decrease in HCV would occur; however, estimates of  $c$  in untreated patients by

apheresis<sup>28</sup> agree with estimates made in IFN- $\alpha$ -treated patients<sup>51</sup>. Analysing data from clinical trials has shown that the reduction in viral production is related to the dose of IFN- $\alpha$ , with 5 MU (million units) given daily yielding a reduction of ~80% in HCV GENOTYPE 1-infected patients, whereas 10 MU given daily yields a reduction of ~95% for HCV genotype 1 and over 99% for HCV genotype 2 (REFS 51,54). An analysis of the kinetics of viral decline showed that at pretreatment, steady-state virus was being produced more rapidly than HIV, with ~10<sup>12</sup> virions/day being generated and cleared, and with free virions having a half-life of 3 hours<sup>51</sup>.

**HBV.** HBV infection has also been modelled using the ‘basic model’<sup>55–57</sup>, and a model<sup>58</sup> including cytokine-mediated ‘cure’ of infected cells<sup>59</sup>. These models indicate that HBV, similar to HIV and HCV, is produced and cleared during chronic infection at a rapid rate, with 10<sup>11</sup>–10<sup>12</sup> virions produced and cleared from plasma per day<sup>55,56</sup>. At the peak of primary HBV infection, 10<sup>13</sup> virions per day are produced<sup>60</sup>. HBV and HCV therapy also yields a two-phase decline in viraemia, with the first phase attributed to virion clearance and the second phase to loss of virus-producing cells by immune-mediated killing<sup>51,55,56</sup> or cytokine-mediated ‘cure’ of infected cells<sup>59</sup>.

**CMV.** The basic model has also been applied to CMV, which has generally been regarded as a slowly replicating virus<sup>61</sup>. Modelling and fitting data from drug-perturbation experiments showed that CMV, similar to HIV, replicates rapidly in its human host with a doubling time of ~1 day<sup>61</sup>, and that the efficacy of ganciclovir, the foremost agent used to treat CMV in the immunocompromised host, is 91.5% when given intravenously, but only 46.5% when given orally<sup>62</sup>. These results have significance for the treatment of CMV and help to explain the appearance of drug-resistant CMV in patients given oral ganciclovir for extended periods<sup>62</sup>.

### Modelling antiviral immune responses

The basic model and a variant containing latently infected cells<sup>63</sup> have been used to model the abrupt rise, peak, subsequent fall, and the establishment of the set-point viral load that characterizes acute HIV infection. It is remarkable that these models do not include an explicit immune response and yet can account for the viral kinetics seen early in infection. To be more specific, in the basic model the rate of infected cell death,  $\delta$ , and the rate of virion clearance,  $c$ , are constants. So, if an immune response had a role in these processes its contribution would need to be small or constant. For example, the rate of death  $\delta$  can be modelled as having two components, one due to viral cytopathic effects ( $\delta_0$ ) and one due to a cell-mediated immune response<sup>64</sup>; for example,  $\delta = \delta_0 + \delta_x X$ , where  $X$  denotes cytotoxic T lymphocytes (CTLs) and  $\delta_x$  the contribution to the rate of infected cell death per CTL. If the total rate of death  $\delta$  is approximately constant, then either  $\delta_x X$  is small compared with  $\delta_0$  or constant. In chronic infection it is easy to predict that the immune response is constant, but

**FOLLICULAR DENDRITIC CELLS (FDCs).** Specialized non-haematopoietic stromal cells that reside in lymphoid follicles and germinal centres. These cells have long dendrites and carry intact antigen on their surface for long periods of time.

**INTERFERON- $\alpha$  (IFN- $\alpha$ ).** A cytokine secreted by many cell types in an early response to viral infection. IFN- $\alpha$  has pleiotropic antiviral effects, including inhibition of protein synthesis and DNA replication, enhanced antigen presentation and natural killer-cell activation.

**HCV GENOTYPE**  
The nucleotide sequence of HCV is highly variable, with the most divergent isolates sharing only 60% nucleotide sequence homology. On the basis of sequence similarity, isolates have been grouped into six main types, called genotypes.

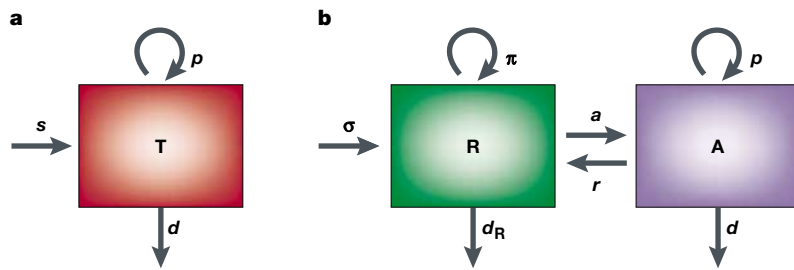


**Figure 2 | Models of T-cell dynamics.** **a** | Basic model in which T cells are supplied by a source,  $s$ , proliferate at rate  $p$  and die at rate  $d$  per cell. **b** | A more realistic model in which T cells can either be resting (R) or activated (A). Resting cells are derived from a source at rate  $\sigma$ , can possibly proliferate very slowly at rate  $\pi$ , die at rate  $d_R$ , and become activated at rate  $a$ . Activated cells proliferate at rate  $p$ , die at rate  $d$ , and return to rest at rate  $r$ . These models have been used to model T-cell dynamics and to interpret labelling experiments (REFS 26,92,93 and R. J. De Boer, H. Mohri, D. D. Ho and A.S.P., unpublished observations).

during primary infection an HIV-specific CTL response is generated and correlates temporally with the decline in viraemia<sup>65</sup>. Therefore, the fact that models with constant  $\delta$  can account for the kinetics of acute HIV infection is surprising. In the basic model, the decline in virus from its peak is due to target-cell limitation — that is, running out of cells to infect<sup>63</sup>.

Stafford *et al.*<sup>66</sup> fit viral-load data from ten primary infection patients and showed that the basic model fit the data well for the first 100 days of infection. However, in some patients, the decline in virus after the peak was more profound than the basic target-cell-limited model could explain. Surprisingly, even when the viral load fell 1–2 orders of magnitude more than predicted by the target-cell-limited model it still obtained a set point consistent with the prediction of the basic model. This suggests that by the time viral loads reach peak values, or slightly after, the immune response might have a role in decreasing viral loads, but that the response is transient, possibly owing to the loss of HIV-specific helper T cells and dysfunction of effector CD8<sup>+</sup> T cells<sup>67,68</sup>. At the moment, these are speculations driven by modelling and limited data, but they present a path for future experiment.

**Responses to acute infection.** For some acutely-infecting viruses, such as LCMV, a CTL response is necessary to clear the infection<sup>69,70</sup>. Mathematical models have been used to describe the kinetics of the CTL response to LCMV<sup>71,72</sup> and suggest the tenfold difference in the magnitude of the response to dominant versus subdominant CTL epitopes might be due to a difference in the epitope concentration needed for half-maximal T-cell stimulation<sup>71</sup>. Models of the kinetics of other acute infections, such as HCV and influenza, are being developed (see REF. 73 and P. Baccam, C. Macken and A.S.P., unpublished observations). Although it has not yet been accomplished, it will be intriguing if one can discern from these modelling efforts the kinetic and immunological factors that differ between viral infections that are cleared and those that become persistent.

Developing models of the antiviral immune response is a substantial challenge. Rather than relying

on measurements of viral load one needs to characterize the humoral, CTL and non-cytolytic CD8<sup>+</sup> T-cell and cytokine (for example, IFN- $\alpha$ ) responses to viral infection. Even with the advent of MHC TETRAMER technology<sup>74</sup> and intracellular cytokine staining, quantitative kinetic data is limited. Furthermore, a better quantitative understanding of the role of CD4<sup>+</sup> T-cell help in generating and maintaining humoral and CD8<sup>+</sup> T-cell responses is needed. Models by Nowak, Wodarz and colleagues<sup>75–77</sup> are a start in this direction, but so far they have not been explicitly matched against experimental data. Substantive collaborations between modellers and experimental groups are needed to further this endeavour.

**Establishing the viral set point.** An interesting theoretical, as well as practical, question is what controls the viral set point in HIV infection? High viral set points are associated with rapid progression to AIDS, whereas low set points are associated with slow progression<sup>25,78</sup>. In the Stafford *et al.*<sup>66</sup> analysis, patients with different set points had various small differences in essentially all of the parameters of the basic model. A more elaborate analysis<sup>79</sup> supports this idea that not one but many parameters control the set point. Despite this, an important set of experiments<sup>80,81</sup> in which CD8<sup>+</sup> T cells were transiently depleted by monoclonal anti-CD8 antibody treatment in simian immunodeficiency virus (SIV)-infected rhesus macaques, showed a 10–10<sup>4</sup>-fold rise in plasma SIV as CD8<sup>+</sup> T cells were lost, and a re-establishment of the set point when the CD8<sup>+</sup> T cells recovered. These experiments strongly indicate that CD8<sup>+</sup> T cells have a role in determining the viral set point. But is this through direct action, such as a CTL response, or by more indirect means? Apart from directly killing virally infected cells, CD8<sup>+</sup> T cells produce  $\beta$ -chemokines that block the entry of certain virions into target cells<sup>82</sup> and inhibitory factors that suppress viral transcription<sup>83</sup> and, hence, efficient production of virions. Using the basic model, we asked whether the marked rise in plasma SIV could be mimicked solely by reducing  $\delta$ <sup>81</sup>. (If  $\delta = \delta_0 + \delta_X X$  and  $X = \text{CTL}$ , then reducing CTL is equivalent to reducing  $\delta$ .) The model predicted a tenfold rise in plasma viraemia over the course of a week, but could not account for the increases of up to 3 or 4 orders of magnitude seen in some macaques. The basic model assumes that virions are made at a constant rate,  $p$ . So, increasing the lifespan of a cell twofold will increase the amount of produced virus twofold, which, in turn, causes some additional cell infections. However, an open question is whether the assumption of constant  $p$  is valid. Some models have assumed that there is a delay between the time of infection and the start of virus production<sup>84–88</sup>, so that  $p$  is initially zero and then jumps to a constant value. Another approach is to assume that after an initial period of no virus production,  $p$  increases with time since infection, ultimately reaching saturation. Models that incorporate this assumption are under development (P. W. Nelson, M. A. Gilchrist and A.S.P., unpublished observations).

**MHC TETRAMERS**  
Reagents composed of four MHC–peptide complexes linked by biotinylation, which can be fluorescently labelled and used to track antigen-specific T cells by flow cytometry.



# Box 2 | Interpreting labelling experiments

Models are needed to interpret bromodeoxyuridine (BrdU)- and deuterated glucose ( $^2\text{H}$ -glucose)-labelling experiments. The simplest model for T-cell population dynamics is shown in FIG. 2a. If  $T$  denotes the population of cells, the equation describing the model is

$$\frac{dT}{dt} = s + (p - d)T \quad (9)$$

When BrdU is present, each unlabelled cell,  $U$ , on division is replaced by two labelled cells,  $L$ . If both labelled and unlabelled cells die at the same rate,  $d$ , then one has:

$$\frac{dU}{dt} = s_U - pU - dU \quad (10)$$

$$\frac{dL}{dt} = s_L + 2pU + (p - d)L \quad (11)$$

where  $s_U$  and  $s_L$  are sources of unlabelled and labelled cells, respectively. If the total number of cells is unchanging and cells are initially unlabelled, with  $U_0$  being the initial number of cells, then the solution of equation (10) can be written as<sup>92</sup>

$$f_L = 1 - U(t)/U_0 = C(1 - e^{-(p+d)t}) \quad (12)$$

where  $f_L$  is the fraction of labelled cells,  $C$  is a constant given by  $C = 1 - s_U/[U_0(p + d)]$ , and  $s_U/U_0$  is the fraction of the total cell population provided by the unlabelled source per unit time. A similar analysis provides the equation describing the decline in  $f_L$  after BrdU is withdrawn<sup>92</sup>. An analysis using the model in FIG. 2b yields similar results<sup>95</sup>.

Modelling  $^2\text{H}$ -glucose labelling is similar, except one now measures the fraction of labelled DNA in a population of cells. So, the appropriate model follows unlabelled,  $U$ , and labelled,  $L$ , DNA strands. When a cell divides in the presence of  $^2\text{H}$ -glucose, the newly synthesized DNA is labelled, but the template DNA remains unchanged. Therefore, on division,  $U \rightarrow U + L$ ,  $L \rightarrow L + L$ . Hence the appropriate model equations for the changes in unlabelled and labelled DNA in the presence of  $^2\text{H}$ -glucose are:

$$\frac{dU}{dt} = s_U - dU \quad (13)$$

$$\frac{dL}{dt} = s_L + pU + (p - d)L \quad (14)$$

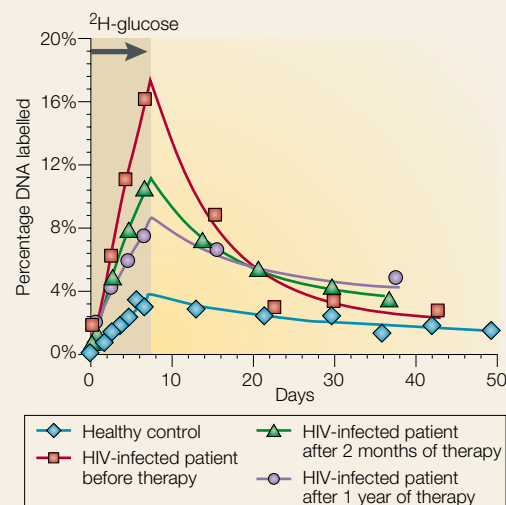
from which one can deduce<sup>93</sup>

$$f_L = 1 - U(t)/U_0 = C(1 - e^{-dt}), \quad (15)$$

where  $C = 1 - s_U/(U_0d)$ . The equation describing the decay of labelled DNA after  $^2\text{H}$ -glucose is withdrawn, which can be derived analogously, is<sup>93</sup>

$$f_L = (f_L(t_e) - s_L'/(U_0d))e^{-d(t-t_e)} + s_L'/(U_0d), \quad (16)$$

where  $t_e$  is the time  $^2\text{H}$ -glucose labelling ends and  $s_L'$  is the source rate of labelled DNA after labelling ends. Analyses based on the model in FIG. 2b give more complex relations, but provide an interpretation for the various source terms<sup>101</sup>. The figure shows the best-fit theoretical curve (solid line) and experimental data from an  $^2\text{H}$ -glucose labelling experiment in which  $^2\text{H}$ -glucose was administered for the first 7 days and then was withdrawn. (Reproduced with permission from REF. 93 © (2001) Rockefeller University Press.)



A related mechanism assumes that activated  $\text{CD8}^+$  T cells produce a factor that normally limits viral production<sup>89</sup>. Then, loss of this factor would increase  $p$ . For example, one might assume  $p = p_0/(1 + aX)$ , where  $X$  is  $\text{CD8}^+$  T cells,  $a$  is a constant proportional to the amount of antiviral factor made per  $\text{CD8}^+$  T cell and  $p_0$  is the rate of virion production in the absence of factor. Using this form of  $p$ , changes of a factor of ten in the plasma virus level can be obtained within 1 day of  $\text{CD8}^+$  T-cell

depletion<sup>81</sup>. However, one complication not yet considered is that increasing virion production might increase viral cytopathicity. Models are an ideal vehicle for examining the quantitative consequences of these competing effects. A lesson from this analysis is that the basic model with constant parameters should only be taken as a starting point and that, as additional quantitative experiments probe the mechanisms of immune system interaction with viruses, elaborations will be needed.

### Modelling lymphocyte dynamics

Modelling the changes in the populations of T cells during immune responses and during HIV infection has provided quantitative information about lymphocyte dynamics, and has helped to elucidate the mechanisms underlying T-cell depletion in HIV-infected patients and the potential for T-cell recovery with potent antiretroviral therapy. T cells are produced in the thymus, they proliferate in the blood and lymphoid tissues and then die (FIG. 2). In the case of HIV infection, cell death is enhanced, but depletion will only occur if the supply of new cells cannot keep pace with the rate of depletion. To fully understand this issue, quantitative measurements of lymphocyte dynamics and models are needed.

One method of obtaining information about cell kinetics is to label cells with agents such as bromodeoxyuridine (BrdU) or deuterated glucose ( $^2\text{H}$ -glucose)<sup>90,91</sup>, which are incorporated into the newly synthesized DNA of dividing cells. Using pulse-chase experiments, the kinetics of the acquisition and loss of labelled cells can be followed<sup>92–94</sup>. Interestingly, a mathematical model is crucial for extracting quantitative information from labelling experiments. For example, one might mistakenly interpret the rate at which a population of cells acquires BrdU as the rate of cell proliferation,  $p$ , and the rate of loss of BrdU-labelled cells after BrdU is withdrawn as the rate of cell death,  $d$ . Flow cytometry is used to measure  $f_L$ , the fraction of BrdU-labelled cells in a population. Modelling shows that the rate at which  $f_L$  increases is indicative of the sum of the proliferation and death rates, whereas the rate of decay during the BrdU-free chase reflects the death rate minus the proliferation rate<sup>95</sup>. The reason for this can be seen by considering unlabelled cells, which decrease by death or by proliferating and acquiring label. As the fraction of labelled cells  $f_L$  is one minus the fraction of unlabelled cells,  $f_L$  increases at a rate proportional to  $d + p$  (BOX 2). The interpretation of  $^2\text{H}$ -glucose-labelling experiments is different because the fraction of labelled DNA from a population of cells is measured rather than the fraction of labelled cells; however, models (BOX 2) are still needed to extract parameters from experimental data<sup>93</sup>.

With models and labelling experiments at hand, what have we learned? First, in HIV-infection  $\text{CD4}^+$  T-lymphocyte depletion can be due to increased cellular destruction, decreased production, or both. In terms of the simple model in BOX 2, the rate of death,  $d$ , can increase and/or the rate of production from source,  $s$ , or proliferation,  $p$ , can decrease.

For a population that is not changing rapidly — that is, in quasi-steady state — the rate of loss from death must match the production from source and proliferation; therefore, the rate of death can be used as a measure of the turnover of the population. Ho *et al.*<sup>18</sup> suggested that HIV is a high-turnover disease, in which the regenerative capacity of T cells at some point fails to keep up with HIV-induced death. Others have suggested that HIV is characterized by a failure in T-cell production<sup>96</sup>. Using the model in BOX 2, the parameters  $p$ ,  $d$  and  $s$  for uninfected controls, SIV-infected macaques<sup>92</sup> and HIV-infected patients have been estimated<sup>93</sup>. Although the model and

its interpretation in the case of BrdU labelling raised some concerns — due to possible label dilution<sup>97</sup> and heterogeneity in populations<sup>98</sup>, which can be resolved by estimating the average turnover of all populations (R. J. De Boer, H. Mohri, D. D. Ho and A. S. P., unpublished observations) — the results with  $^2\text{H}$ -glucose labelling are clear cut. Mean proliferation and death rates of  $\text{CD4}^+$  T cells are elevated threefold or more with HIV-infection, but subsequently reduce to nearly normal levels after 1 year of antiretroviral therapy<sup>93</sup>. These quantitative results strongly indicate that the  $\text{CD4}^+$  lymphocyte depletion observed in AIDS is primarily a consequence of increased cellular destruction, and not decreased production.

### Concluding remarks

Models provide a rigorous means of thinking about and describing the immune system and its interactions with viruses and other pathogens. As shown here, models can take the form of a picture (for example, FIG. 1) that depicts various processes. A mathematical model goes further and codifies the picture in terms of equations (for example, BOX 1), which can be used to make predictions (for example, if a drug is given viral load will fall according to equation (8) in BOX 1). Testing such a prediction, however, depends on obtaining data and using that data to estimate parameters. Models can also be used to test hypotheses. In the case of the model of HCV infection, one could use the model to predict what would occur if  $\text{IFN-}\alpha$  acted by blocking *de novo* infection, viral replication or if it affected virion clearance. In combination with data, one could then evaluate the various hypotheses. Models also provide a means of calculating things. An example was calculating the likelihood of HIV developing a drug-resistant mutation, given a certain replication rate and mutation rate.

Success in describing HIV and T-cell dynamics has been due, in part, to the availability of reliable highly quantitative data. The willingness of experimental labs to expend considerable resources to produce quantitative rather than qualitative data is partly the result of the early successes of modelling in HIV research. At first glance, it is somewhat surprising that the merging of quantitative theory and experiment came about in the context of clinical rather than basic research in immunology. However, the need to make progress, the resources and prescient collaborators were available. Other areas of immunology involve complicated phenomena that can benefit from quantitative analysis. However, labs need to choose between going after the next molecule or doing quantitative experiments and modelling that hopefully will integrate immunological knowledge into a larger conceptual picture. Although it might be easy to understand how one or a few molecules influence an immune response, understanding the simultaneous effects of tens or hundreds of molecules requires a quantitative description. Theory, which is distinct from modelling, need not be mathematical, as evidenced by clonal selection, and drives much experimentation. To some extent all immunologists act as theorists when designing and interpreting experiments.

However, new technologies, such as microarrays, protein chips, powerful computers and databases, are increasing the amount of information one has available. This is changing the way all of biology is done and leading to increased emphasis on a systems level biology. Large-scale computational models of the immune

system<sup>10,99,100</sup> might one day pave the way to an integration of the growing body of immunological information. At the moment, however, the field of theoretical immunology is being built model by model. Additional collaborations between bench immunologists and mathematical modellers are sorely needed.

1. Perelson, A. S. & Weisbuch, G. Immunology for physicists. *Rev. Mod. Phys.* **69**, 1219–1267 (1997).
2. Perelson, A. S. & Oster, G. F. Theoretical studies of clonal selection: minimal antibody repertoire size and reliability of self-non-self discrimination. *J. Theor. Biol.* **81**, 645–670 (1979).
3. Perelson, A. S. in *Cell Surface Dynamics: Concepts and Models* (eds Perelson, A. S., DeLisi, C. & Weigel, F. W.) 223–276 (Marcel Dekker, New York, 1984).
4. Kepler, T. B. & Perelson, A. S. Cyclic re-entry of germinal center B cells and the efficiency of affinity maturation. *Immunol. Today* **14**, 412–415 (1993).
5. De Boer, R. J. & Perelson, A. S. How diverse should the immune system be? *Proc. R. Soc. Lond. B* **252**, 171–175 (1993).
6. Percus, J. K., Percus, O. E. & Perelson, A. S. Predicting the size of the T-cell receptor and antibody combining region from consideration of efficient self-nonself discrimination. *Proc. Natl Acad. Sci. USA* **90**, 1691–1695 (1993).
7. McKeithan, T. W. Kinetic proofreading in T-cell receptor signal transduction. *Proc. Natl Acad. Sci. USA* **92**, 5042–5046 (1995).
8. McLean, A. R., Rosado, M. M., Agenes, F., Vasconcellos, R. & Freitas, A. A. Resource competition as a mechanism for B cell homeostasis. *Proc. Natl Acad. Sci. USA* **94**, 5792–5797 (1997).
9. Borghans, J. A., De Boer, R. J., Sercarz, E. & Kumar, V. T cell vaccination in experimental autoimmune encephalomyelitis: a mathematical model. *J. Immunol.* **161**, 1087–1093 (1998).
10. Smith, D. J., Forrest, S., Ackley, D. H. & Perelson, A. S. Variable efficacy of repeated annual influenza vaccination. *Proc. Natl Acad. Sci. USA* **96**, 14001–14006 (1999).
11. Shows, through a large-scale simulation model of the humoral immune response, that variable efficacy of influenza vaccine in repeat vaccinees can be explained by a memory response to a prior vaccine or infection; that is, original antigenic sin.
12. Detours, V. & Perelson, A. S. Explaining high alloreactivity as a quantitative consequence of affinity-driven thymocyte selection. *Proc. Natl Acad. Sci. USA* **96**, 5153–5158 (1999).
13. Keshmir, C. & De Boer, R. J. A mathematical model on germinal center kinetics and termination. *J. Immunol.* **163**, 2463–2469 (1999).
14. Borghans, J. A., Taams, L. S., Wauben, M. H. & de Boer, R. J. Competition for antigenic sites during T cell proliferation: a mathematical interpretation of *in vitro* data. *Proc. Natl Acad. Sci. USA* **96**, 10782–10787 (1999).
15. Borghans, J. A., Noest, A. J. & De Boer, R. J. How specific should immunological memory be? *J. Immunol.* **163**, 569–575 (1999).
16. Segel, L. A. & Bar-Or, R. L. On the role of feedback in promoting conflicting goals of the adaptive immune system. *J. Immunol.* **163**, 1342–1349 (1999).
17. Detours, V. & Perelson, A. S. The paradox of alloreactivity and self MHC restriction: quantitative analysis and statistics. *Proc. Natl Acad. Sci. USA* **97**, 8479–8483 (2000).
18. Hlavacek, W. S., Redondo, A., Metzger, H., Wofsy, C. & Goldstein, B. Kinetic proofreading models for cell signaling predict ways to escape kinetic proofreading. *Proc. Natl Acad. Sci. USA* **98**, 7295–7300 (2001).
19. Ho, D. D. *et al.* Rapid turnover of plasma virions and CD4 lymphocytes in HIV-1 infection. *Nature* **373**, 123–126 (1995).
20. Wei, X. *et al.* Viral dynamics in human immunodeficiency virus type 1 infection. *Nature* **373**, 117–122 (1995).
21. References 18 and 19 are the key papers showing that HIV replicates and is cleared rapidly during chronic HIV-1 infection.
22. Perelson, A. S., Neumann, A. U., Markowitz, M., Leonard, J. M. & Ho, D. D. HIV-1 dynamics *in vivo*: virion clearance rate, infected cell life-span, and viral generation time. *Science* **271**, 1582–1586 (1996).
23. This paper provided estimates of the lifespan of productively infected CD4<sup>+</sup> lymphocytes and the rate of clearance of free virions.
24. Coffin, J. M. HIV population dynamics *in vivo*: implications for genetic variation, pathogenesis, and therapy. *Science* **267**, 483–489 (1995).
25. Wain-Hobson, S. AIDS. Virological mayhem. *Nature* **373**, 102 (1995).
26. Perelson, A. S., Essunger, P. & Ho, D. D. Dynamics of HIV-1 and CD4<sup>+</sup> lymphocytes *in vivo*. *AIDS* **11**, S17–S24 (1997).
27. Nowak, M. A. & May, R. M. *Virus Dynamics: Mathematical Principles of Immunology and Virology* (Oxford Univ. Press, 2000).
28. Monograph that reviews the field of viral dynamic modelling.
29. Ho, D. D. Viral counts count in HIV infection. *Science* **272**, 1124–1125 (1996).
30. Perelson, A. S. & Nelson, P. W. Mathematical analysis of HIV-1 dynamics *in vivo*. *SIAM Rev.* **41**, 3–44 (1999).
31. A review of the mathematics used in modelling HIV infection.
32. Wu, H., Ruan, P., Ding, A. A., Sullivan, J. L. & Luzuriaga, K. Inappropriate model-fitting methods may lead to significant underestimates of viral decay rates in HIV dynamic studies. *J. Acquir. Immune Defic. Syndr.* **21**, 426–428 (1999).
33. Ramratnam, B. *et al.* Rapid production and clearance of HIV-1 and hepatitis C virus assessed by large volume plasma apheresis. *Lancet* **354**, 1782–1785 (1999).
34. Mansky, L. M. & Temin, H. M. Lower *in vivo* mutation rate of human immunodeficiency virus type 1 than that predicted from the fidelity of purified reverse transcriptase. *J. Virol.* **69**, 5087–5094 (1995).
35. Bonhoeffer, S., May, R. M., Shaw, G. M. & Nowak, M. A. Virus dynamics and drug therapy. *Proc. Natl Acad. Sci. USA* **94**, 6971–6976 (1997).
36. Wein, L. M., D'Amato, R. M. & Perelson, A. S. Mathematical analysis of antiretroviral therapy aimed at HIV-1 eradication or maintenance of low viral loads. *J. Theor. Biol.* **192**, 81–98 (1998).
37. Ding, A. A. & Wu, H. Relationships between antiviral treatment effects and biphasic viral decay rates in modeling HIV dynamics. *Math. Biosci.* **160**, 63–82 (1999).
38. Mueller, B. U. *et al.* Individual prognoses of long-term responses to antiretroviral treatment based on virological, immunological and pharmacological parameters measured during the first week under therapy. *AIDS* **12**, F191–F196 (1998).
39. Mittler, J. *et al.* Short-term measures of relative efficacy predict longer-term reductions in human immunodeficiency virus type 1 RNA levels following zidovudine monotherapy. *Antimicrob. Agents Chemother.* **45**, 1438–1443 (2001).
40. Louie, M. *et al.* Using viral dynamics to document the greater antiviral potency of a regime containing lopinavir/ritonavir, efavirenz, tenofovir, and lamivudine relative to standard therapy. *8th Conf. Retroviruses Opportunistic Infect. Abstr.* 383 (2001).
41. Perelson, A. S. *et al.* Decay characteristics of HIV-1-infected compartments during combination therapy. *Nature* **387**, 188–191 (1997).
42. This paper reported that the decline in plasma HIV-1 RNA after the initiation of therapy has two phases. The second phase was attributed to long-lived infected cells, release of virus from tissue reservoirs, or the activation of latently infected cells. Indicates that the cells responsible for the second phase could be eradicated after 2–3 years of 100% effective therapy.
43. Finzi, D. *et al.* Identification of a reservoir for HIV-1 in patients on highly active antiretroviral therapy. *Science* **278**, 1295–1300 (1997).
44. Chun, T. W. *et al.* Quantification of latent tissue reservoirs and total body viral load in HIV-1 infection. *Nature* **387**, 183–188 (1997).
45. Zhang, L. *et al.* Quantifying residual HIV-1 replication in patients receiving combination antiretroviral therapy. *N. Engl. J. Med.* **340**, 1605–1613 (1999).
46. Finzi, D. *et al.* Latent infection of CD4<sup>+</sup> T cells provides a mechanism for lifelong persistence of HIV-1, even in patients on effective combination therapy. *Nature Med.* **5**, 512–517 (1999).
47. Wong, J. K. *et al.* Recovery of replication-competent HIV despite prolonged suppression of plasma viremia. *Science* **278**, 1291–1295 (1997).
48. Chun, T. W. *et al.* Presence of an inducible HIV-1 latent reservoir during highly active antiretroviral therapy. *Proc. Natl Acad. Sci. USA* **94**, 13193–13197 (1997).
49. Furtado, M. R. *et al.* Persistence of HIV-1 transcription in peripheral-blood mononuclear cells in patients receiving potent antiretroviral therapy. *N. Engl. J. Med.* **340**, 1614–1622 (1999).
50. Dornadula, G. *et al.* Residual HIV-1 RNA in blood plasma of patients taking suppressive highly active antiretroviral therapy. *J. Am. Med. Assoc.* **282**, 1627–1632 (1999).
51. Sharkey, M. E. *et al.* Persistence of episomal HIV-1 infection intermediates in patients on highly active anti-retroviral therapy. *Nature Med.* **6**, 76–81 (2000).
52. Siliciano, J. D. & Siliciano, R. F. Latency and viral persistence in HIV-1 infection. *J. Clin. Invest.* **106**, 823–825 (2000).
53. Hlavacek, W. S., Wofsy, C. & Perelson, A. S. Dissociation of HIV-1 from follicular dendritic cells during HAART: mathematical analysis. *Proc. Natl Acad. Sci. USA* **96**, 14681–14686 (1999).
54. Shows that complete elimination of HIV-1 from follicular dendritic cells can take as long as a decade if virions do not degrade.
55. Hlavacek, W. S., Stilianakis, N. I., Notermans, D. W., Danner, S. A. & Perelson, A. S. Influence of follicular dendritic cells on decay of HIV during antiretroviral therapy. *Proc. Natl Acad. Sci. USA* **97**, 10966–10971 (2000).
56. Hlavacek, W. S., Stilianakis, N. I. & Perelson, A. S. Influence of follicular dendritic cells on HIV dynamics. *Phil. Trans. R. Soc. Lond. B* **355**, 1051–1058 (2000).
57. Smith, B. A. *et al.* Persistence of infectious HIV on follicular dendritic cells. *J. Immunol.* **166**, 690–696 (2001).
58. Neumann, A. U. *et al.* Hepatitis C viral dynamics *in vivo* and the antiviral efficacy of interferon- $\alpha$  therapy. *Science* **282**, 103–107 (1998).
59. Shows that HCV, like HIV, has rapid production and clearance. Also indicates that interferon causes rapid HCV clearance mainly by blocking production of virions from infected cells in a dose-dependent manner.
60. Bekker, F. C. *et al.* Ultrarapid hepatitis C virus clearance by daily high-dose interferon in non-responders to standard therapy. *J. Hepatol.* **28**, 960–964 (1998).
61. Yasui, K. *et al.* Dynamics of hepatitis C viremia following interferon- $\alpha$  administration. *J. Infect. Dis.* **177**, 1475–1479 (1998).
62. Neumann, A. U. *et al.* Differences in viral dynamics between genotypes 1 and 2 of hepatitis C virus. *J. Infect. Dis.* **182**, 28–35 (2000).
63. Nowak, M. A. *et al.* Viral dynamics in hepatitis B virus infection. *Proc. Natl Acad. Sci. USA* **93**, 4398–4402 (1996).
64. First paper to analyse the dynamics of HBV infection.
65. Tsiang, M., Rooney, J. F., Toole, J. J. & Gibbs, C. S. Biphasic clearance kinetics of hepatitis B virus from patients during adefovir dipivoxil therapy. *Hepatology* **29**, 1863–1869 (1999).
66. Lau, G. K. *et al.* Combination therapy with lamivudine and famciclovir for chronic hepatitis B-infected Chinese patients: a viral dynamics study. *Hepatology* **32**, 394–399 (2000).
67. Lewin, S. R. *et al.* Analysis of hepatitis B viral load decline under potent therapy: complex decay profiles observed. *Hepatology* **34**, 1012–1020 (2001).
68. Guidotti, L. G. *et al.* Viral clearance without destruction of infected cells during acute HBV infection. *Science* **284**, 825–829 (1999).
69. Whalley, S. A. *et al.* Kinetics of acute hepatitis B virus infection in humans. *J. Exp. Med.* **193**, 847–854 (2001).
70. Emery, V. C., Cope, A. V., Bowen, E. F., Gor, D. & Griffiths, P. D. The dynamics of human cytomegalovirus replication *in vivo*. *J. Exp. Med.* **190**, 177–182 (1999).
71. Emery, V. C. & Griffiths, P. D. Prediction of cytomegalovirus load and resistance patterns after antiviral chemotherapy. *Proc. Natl Acad. Sci. USA* **97**, 8039–8044 (2000).
72. Phillips, A. N. Reduction of HIV concentration during acute infection: independence from a specific immune response. *Science* **271**, 497–499 (1996).



64. Nowak, M. A. & Bangham, C. R. Population dynamics of immune responses to persistent viruses. *Science* **272**, 74–79 (1996).
65. Koup, R. A. *et al.* Temporal association of cellular immune responses with the initial control of viremia in primary human immunodeficiency virus type 1 syndrome. *J. Virol.* **68**, 4650–4655 (1994).
66. Stafford, M. A. *et al.* Modeling plasma virus concentration during primary HIV infection. *J. Theor. Biol.* **203**, 285–301 (2000).
67. Welsh, R. M. Assessing CD8 T cell number and dysfunction in the presence of antigen. *J. Exp. Med.* **193**, F19–F22 (2001).
68. Xiong, Y. *et al.* Simian immunodeficiency virus (SIV) infection of a rhesus macaque induces SIV-specific CD8<sup>+</sup> T cells with a defect in effector function that is reversible on extended interleukin-2 incubation. *J. Virol.* **75**, 3028–3033 (2001).
69. Ahmed, R., Salmi, A., Butler, L. D., Chiller, J. M. & Oldstone, M. B. Selection of genetic variants of lymphocytic choriomeningitis virus in spleens of persistently infected mice. Role in suppression of cytotoxic T lymphocyte response and viral persistence. *J. Exp. Med.* **160**, 521–540 (1984).
70. Walsh, C. M. *et al.* Immune function in mice lacking the perforin gene. *Proc. Natl Acad. Sci. USA* **91**, 10854–10858 (1994).
71. DeBoer, R. J. *et al.* Recruitment times, proliferation, and apoptosis rates during the CD8<sup>+</sup> T cell response to LCMV. *J. Virol.* **75**, 10663–10669 (2001).
72. Bocharov, G. A. Modelling the dynamics of LCMV infection in mice: conventional and exhaustive CTL responses. *J. Theor. Biol.* **192**, 283–308 (1998).
73. Dahari, H., Major, M., Mihalik, K., Feinstone, S. & Neumann, A. U. Lack of virus cytopathicity but strong IFN and cellular immune responses during primary HCV infections in chimpanzees. *Hepatology* **32**, 302A (2000).
74. Altman, J. D. *et al.* Phenotypic analysis of antigen-specific T lymphocytes. *Science* **274**, 94–96 (1996).
75. Wodarz, D. *et al.* A new theory of cytotoxic T-lymphocyte memory: implications for HIV treatment. *Phil. Trans. R. Soc. Lond. B* **355**, 329–343 (2000).
76. Wodarz, D. & Nowak, M. A. Correlates of cytotoxic T-lymphocyte-mediated virus control: implications for immunosuppressive infections and their treatment. *Phil. Trans. R. Soc. Lond. B* **355**, 1059–1070 (2000).
77. Wodarz, D. & Jansen, V. A. The role of T cell help for anti-viral CTL responses. *J. Theor. Biol.* **211**, 419–432 (2001).
78. Mellors, J. W. *et al.* Prognosis in HIV-1 infection predicted by the quantity of virus in plasma. *Science* **272**, 1167–1170 (1996).
79. Muller, V., Maree, A. F. M. & De Boer, R. J. Small variations in multiple parameters account for wide variations in HIV-1 set points: a novel modelling approach. *Proc. R. Soc. Lond. B* **268**, 235–242 (2000).
80. Schmitz, J. E. *et al.* Control of viremia in simian immunodeficiency virus infection by CD8<sup>+</sup> lymphocytes. *Science* **283**, 857–860 (1999).
81. Jin, X. *et al.* Dramatic rise in plasma viremia after CD8<sup>+</sup> T cell depletion in simian immunodeficiency virus-infected macaques. *J. Exp. Med.* **189**, 991–998 (1999).
82. Cocchi, F. *et al.* Identification of RANTES, MIP-1 $\alpha$ , and MIP-1 $\beta$  as the major HIV- suppressive factors produced by CD8<sup>+</sup> T cells. *Science* **270**, 1811–1815 (1995).
83. Mackewicz, C. E., Blackbourn, D. J. & Levy, J. A. CD8<sup>+</sup> T cells suppress human immunodeficiency virus replication by inhibiting viral transcription. *Proc. Natl Acad. Sci. USA* **92**, 2308–2312 (1995).
84. Herz, A. V., Bonhoeffer, S., Anderson, R. M., May, R. M. & Nowak, M. A. Viral dynamics *in vivo*: limitations on estimates of intracellular delay and virus decay. *Proc. Natl Acad. Sci. USA* **93**, 7247–7251 (1996).
85. Mittler, J. E., Sulzer, B., Neumann, A. U. & Perelson, A. S. Influence of delayed viral production on viral dynamics in HIV-1 infected patients. *Math. Biosci.* **152**, 143–163 (1998).
86. Mittler, J. E., Markowitz, M., Ho, D. D. & Perelson, A. S. Improved estimates for HIV-1 clearance rate and intracellular delay. *AIDS* **13**, 1415–1417 (1999).
87. Nelson, P. W., Murray, J. D. & Perelson, A. S. A model of HIV-1 pathogenesis that includes an intracellular delay. *Math. Biosci.* **163**, 201–215 (2000).
88. Nelson, P. W., Mittler, J. E. & Perelson, A. S. Effect of drug efficacy and the eclipse phase of the viral life cycle on estimates of HIV viral dynamic parameters. *J. Acquir. Immune Defic. Syndr.* **26**, 405–412 (2001).
89. Levy, J. A. *HIV and the Pathogenesis of AIDS* (American Society for Microbiology, Washington DC, 1998).
90. Macallan, D. C. *et al.* Measurement of cell proliferation by labeling of DNA with stable isotope-labeled glucose: studies *in vitro*, in animals, and in humans. *Proc. Natl Acad. Sci. USA* **95**, 708–713 (1998).
91. Hellerstein, M. K. Measurement of T-cell kinetics: recent methodologic advances. *Immunol. Today* **20**, 438–441 (1999).
92. Mohri, H., Bonhoeffer, S., Monard, S., Perelson, A. S. & Ho, D. D. Rapid turnover of T lymphocytes in SIV-infected rhesus macaques. *Science* **279**, 1223–1227 (1998).
93. Mohri, H. *et al.* Increased turnover of T lymphocytes in HIV-1 infection and its reduction by antiretroviral therapy. *J. Exp. Med.* **194**, 1277–1287 (2001).
- T-cell kinetics in uninfected and HIV-infected humans determined by stable isotope labelling and modelling of the labelling kinetics.**
94. McCune, J. M. *et al.* Factors influencing T-cell turnover in HIV-1-seropositive patients. *J. Clin. Invest.* **105**, R1–R8 (2000).
95. Bonhoeffer, S., Mohri, H., Ho, D. & Perelson, A. S. Quantification of cell turnover kinetics using 5-bromo-2'-deoxyuridine. *J. Immunol.* **164**, 5049–5054 (2000).
96. Hellerstein, M. *et al.* Directly measured kinetics of circulating T lymphocytes in normal and HIV-1-infected humans. *Nature Med.* **5**, 83–89 (1999).
97. Rouzine, I. M. & Coffin, J. M. T cell turnover in SIV infection. *Science* **284**, 555b (1999).
98. Grossman, Z., Herberman, R. B. & Dimitrov, D. S. T cell turnover in SIV infection. *Science* **284**, 555a (1999).
99. Celada, F. & Seiden, P. E. A computer model of cellular interactions in the immune system. *Immunol. Today* **13**, 56–62 (1992).
100. Smith, D. J., Forrest, S., Ackley, D. H. & Perelson, A. S. Using lazy evaluation to simulate realistic-size repertoires in models of the immune system. *Bull. Math. Biol.* **60**, 647–658 (1998).
101. Ribiero, R., Mohri, H., Ho, D. D. & Perelson, A. S. Modeling deuterated glucose labeling of T lymphocytes. *Bull. Math. Biol.* (in the press).

## Acknowledgements

This work was supported by the US Department of Energy and the National Institutes of Health. I thank R. Ribeiro for helpful comments.

## Online Links

### DATABASES

The following terms in this article are linked online to:

**LocusLink:** <http://www.ncbi.nlm.nih.gov/LocusLink/>

IFN- $\alpha$

**Medscape DrugInfo:**

<http://promini.medscape.com/drugdb/search.asp>  
ganciclovir | ritonavir

### FURTHER INFORMATION

**Encyclopedia of life sciences:** <http://www.els.net>  
bioinformatics | cytomegalovirus infections in humans | hepatitis B virus | hepatitis C virus | human immunodeficiency virus (HIV)

**HIV Molecular Immunology Database:**

[www.hiv.lanl.gov/immunology](http://www.hiv.lanl.gov/immunology)

**HIV Sequence Database:** [www.hiv.lanl.gov/](http://www.hiv.lanl.gov/)

**Access to this interactive links box is free online.**